

# Unveiling the Inner Disk Structure of T Tauri Stars

James Muzerolle <sup>1</sup>, Nuria Calvet <sup>2</sup>, Lee Hartmann <sup>2</sup>, and Paola D'Alessio<sup>3</sup>

## ABSTRACT

We present near-infrared spectra of the excess continuum emission from the innermost regions of classical T Tauri disks. In almost all cases, the shape of the excess is consistent with that of a single-temperature blackbody with  $T \sim 1400$  K, similar to the expected dust sublimation temperature for typical dust compositions. The amount of excess flux roughly correlates with the accretion luminosity in objects with similar stellar properties. We compare our observations with the predictions of simple disk models having an inner rim located at the dust sublimation radius, including irradiation heating of the dust from both the stellar *and* accretion luminosities. The models yield inner rim radii in the range 0.07-0.54 AU, increasing with higher stellar and accretion luminosities. Using typical parameters which fit our observed sample, we predict a rim radius  $\sim 0.2$  AU for the T Tauri star DG Tau, which agrees with recent Keck near-infrared interferometric measurements. For large mass accretion rates, the inner rim lies beyond the corotation radius at (or within) which magnetospheric accretion flows are launched, which implies that pure gaseous disks must extend inside the dust rim. Thus, for a significant fraction of young stars, dust cannot exist in the innermost disk, calling into question theories in which solid particles are ejected by a wind originating at the magnetospheric radius.

*Subject headings:* accretion — stars: pre-main sequence — stars: formation — infrared: stars — techniques: spectroscopic

---

<sup>1</sup>Steward Observatory, University of Arizona, 933 N. Cherry Ave., Tucson, AZ 85721 (jamesm@as.arizona.edu)

<sup>2</sup>Harvard-Smithsonian Center for Astrophysics, Mail Stop 42, 60 Garden Street, Cambridge, MA 02138 (ncalvet@cfa.harvard.edu, hartmann@cfa.harvard.edu)

<sup>3</sup>Instituto de Astronomía, UNAM, Ap. Postal 3-72, 58089 Morelia, México (p.dalessio@astrosmo.unam.mx)

## 1. Introduction

The structure of inner disk regions of classical T Tauri stars (CTTSs) has important consequences for both the transfer of material to the star and the processing of solid material in the terrestrial planet region. It is now generally accepted that the accretion of disk material onto the central star is channeled by the stellar magnetosphere. The inner edge of the disk is truncated by the stellar magnetic field at or inside the corotation radius, where the disk rotates at the same angular velocity as the star (e.g., Shu et al. 1994), typically a few stellar radii from the stellar surface. Gas from the disk is channeled out of the disk plane along magnetic field lines to impact the stellar surface in an accretion shock. Observations and modeling of both permitted emission line profiles produced in the infalling gas streams (Muzerolle, Hartmann, & Calvet 2001, and references therein) and hot continuum excess produced by the accretion shock (Calvet & Gullbring 1998) lend strong support to this picture.

However, substantial uncertainty remains concerning the detailed structure of the disk near the inner truncation radius. Meyer, Calvet, & Hillenbrand (1997: MCH97) showed that the near-infrared excess emission of CTTSs, which arises from inner disk regions, is correlated with accretion rate. However, quantitative agreement with standard disk models required accretion rates higher by a factor of  $\sim 10$  than subsequently estimated from UV excess emission (e.g., Gullbring et al. 1998). Recent determinations of near-infrared continuum excesses or “veiling” also showed larger disk emission than predicted by simple models (Folha & Emerson 1999); Johns-Krull & Valenti (2001) found that disk models such as those of Chiang & Goldreich (1997, 1999) and D’Alessio et al. (1998) underestimated the  $K$ -band veiling by factors of up to  $\sim 2$ -3.

The higher mass Herbig Ae/Be stars (HAEBESs) also show large near-infrared excesses difficult to explain with simple accretion disk models (Hillenbrand et al. 1992; Hartmann, Kenyon, & Calvet 1993). Natta et al. (2001) attempted to solve this problem by postulating that the near-infrared emission arises from an inner disk rim at the dust destruction radius. The rim is “puffed” because of the normal incidence of the stellar radiation, which is the primary source of dust heating. At the same time, Tuthill et al. (2001) independently proposed dust sublimation to describe the near-infrared interferometric size for the HAEBES LkH $\alpha$  101. Other recent near-infrared interferometric observations of HAEBESs have resolved structures with sizes and visibilities in qualitative agreement with the puffed rim picture (Millan-Gabet, Schloerb, & Traub 2001; Eisner et al. 2003). A similar inner dust rim in CTTSs seems likely; an inner edge must already exist near the corotation radius by magnetic truncation, and dust cannot survive inside this radius.

To investigate this possibility, we have obtained 2-5  $\mu\text{m}$  spectra of a sample of well-

studied CTTSs. These spectra, with simultaneous coverage over a wide wavelength range, provide a far more sensitive probe of the shape and strength of the excess emission than previous photometric measurements. Unlike HAEBESs, the near-infrared continuum excesses of CTTSs do not stand out strongly in contrast with the stellar photosphere. The only way to disentangle the two broad continua (with less dissimilar characteristic temperatures) is to determine the spectrum of the excess by measuring absorption line veiling from high-quality spectra simultaneously spanning a large range of wavelength. We show that the excess spectra derived from our data appear to be dominated by a single-temperature blackbody component with characteristic temperature roughly corresponding to the dust sublimation limit. We then compute models for an inner dust rim, from which we can estimate the dust truncation radii,  $R_d$ .

## 2. Spectra of the Infrared Excess

We observed a sample of 9 CTTSs with SpeX on IRTF (Rayner et al. 1998) during the nights of January 5-6, 2001. Each spectrum we observed spans a wavelength range of about 2.1-4.8  $\mu\text{m}$ , which contains multiple hydrogen emission lines that serve as key accretion diagnostics (see §3), and  $K$ -band atomic absorption features that can be used to measure continuum veiling of the stellar photosphere from disk emission. We selected a representative sample of pre-main sequence objects, spanning a wide range of stellar and accretion properties. These objects have been studied extensively, and the stellar parameters are well-determined (see Table 1), with the exception of DR Tau, the most active object with the largest amount of optical continuum excess.

Most of the basic data reduction steps were performed using the facility IDL extraction software “Spextool” (Cushing et al. 2003). Removal of telluric absorption lines was done separately; each object spectrum was divided by a solar-type dwarf standard spectrum taken at a similar airmass and sky position, and then multiplied by the solar spectrum to remove residuals from photospheric features in the standard spectrum. Spectra from each order (6 orders in all) were then pieced together into one final spectrum for each object. The overall continuum level across all the orders is remarkably consistent, with generally good agreement in the regions of order overlap.

We measured the veiling at 2.2  $\mu\text{m}$  ( $r_{2.2} = F_{excess,2.2}/F_{*,2.2}$ ) by comparing each object spectrum with a weak T Tauri or dwarf template spectrum of similar spectral type, after normalizing all the spectra by the observed flux at the shortest wavelength (roughly 2.12  $\mu\text{m}$ ). The template spectra were then artificially veiled by adding an excess continuum until the depth of photospheric features around 2.2  $\mu\text{m}$  matched the depth of the features in the

object spectra. The measured veilingings are listed in Table 1. These are in relative agreement with previous determinations from high-resolution spectra (Folha & Emerson 1999; Johns-Krull & Valenti 2001). Since the data are not absolutely flux calibrated, we used the veiling values to scale the object spectra relative to the unveiled template spectra. Both object and template spectra were dereddened using published  $A_V$  values. Finally, excess spectra were created by subtracting each dereddened, veiling-scaled object spectrum by the appropriate dereddened template spectrum.

The resultant excess spectra are shown in Figure 1. The excess flux appears to increase with wavelength through the  $K$ -band, but turns over between 2.5 - 3  $\mu\text{m}$  (with the exception of DQ Tau, where the flux increases with wavelength throughout the observed range). The spectral shape implies emission from optically thick material at a characteristic temperature; we were able to qualitatively match the shapes using single-temperature blackbodies with  $T \sim 1200 - 1400 \text{ K}$ . These temperatures are close to the dust sublimation limit. We next explore models of emission from an accretion disk with a puffed inner rim corresponding to the dust destruction radius.

### 3. Models

Our model of the inner disk rim will be presented in more detail in a forthcoming paper; see also D’Alessio et al. (2003) for further explanation of the radiative transfer, as well as other comparisons with observed spectral energy distributions. Here, we briefly summarize the main points of the model. We assume that a star of effective temperature, radius, mass, and luminosity given by  $T_*$ ,  $R_*$ ,  $M_*$ , and  $L_*$  is surrounded by a disk, accreting at a rate  $\dot{M}$ , which has a rim at the radius where dust sublimates. For simplicity, we assume this rim to be vertical, even though radial and vertical gradients of density and temperature probably result in a more rounded shape. Our models include a rim atmosphere allowing for the transition from optically-thin to optically-thick absorption and emission. The rim is illuminated by both the star and by radiation emerging from the accretion shock where most of the accretion luminosity  $L_{acc} = GM_*\dot{M}/R_*$  is dissipated (Calvet & Gullbring 1998).

We follow the treatment of Calvet et al. (1991, 1992=CMPD) to describe the temperature structure in the rim atmosphere, extended to include scattering of radiation at the disk characteristic wavelength; we also use the forward scattering approximation, which amounts to taking negligible albedo in the CMPD treatment. The temperature at the top of the rim atmosphere, located at radius  $R$ , is given by

$$T(0)^4 = \frac{E_0}{4\sigma_R} \left( 2 + q \frac{\chi_d}{\kappa_d} \right) \quad (1)$$

where  $E_0 = (L_* + L_{acc})/4\pi R^2$ , and the temperature at the level  $\tau_d \sim 2/3$  is

$$T(2/3)^4 = T_{eff}^4 = \frac{E_0}{4\sigma_R} \left[ 2 + \frac{3}{q} + \left( q \frac{\chi_d}{\kappa_d} - \frac{3}{q} \right) e^{-2q/3} \right]. \quad (2)$$

In these equations,  $q$  is an efficiency factor, given by the ratio of opacities at wavelengths characteristic of the absorption and emission of radiation by the dust in the rim (CMPD), i.e.,  $q = \bar{\kappa}^i / \chi^d$ , where  $\bar{\kappa}^i = (L_* \kappa^* + L_{acc} \kappa^{acc}) / (L_* + L_{acc})$ . In these equations,  $\chi$  refers to the total opacity and  $\kappa$  to the true opacity, each at a wavelength characteristic of the dust in the disk rim (subindex  $d$ ) and of the incident radiation (subindex  $i$ ), in turn composed of stellar ( $\kappa^*$ ) and accretion shock ( $\kappa^{acc}$ ) radiation. In practice,  $\chi$  and  $\kappa$  are means of the monochromatic opacity weighted by blackbodies at  $T_d$ ,  $T_*$ , and  $T_{acc}$ , for the three characteristic radiation fields. We take  $T_{acc} = 8000$  K (Calvet & Gullbring 1998). The rim is then located at radius

$$R_d = \left[ \left( \frac{L_* + L_{acc}}{16\pi\sigma_R} \right) \left( 2 + q \frac{\chi_d}{\kappa_d} \right) \right]^{1/2} \frac{1}{T_d^2} \quad (3)$$

where we have assumed that the thickness of the atmosphere is negligible compared to the radius.

We calculate the scale height of the rim,  $H$ , using eq.(2). The physical height of the rim,  $z_{rim}$ , is then calculated using the expression in Muzerolle et al. (2003) with a central density given by  $\rho_c \sim \Sigma / \sqrt{2\pi} H$ , where the surface density  $\Sigma = \dot{M} / 6\pi\nu [(1 - (R_*/R_d)^{1/2})]$ , and the mass accretion rate  $\dot{M}$  is derived from  $L_{acc}$ . The viscosity is given by  $\nu = \alpha c_s (T_{eff})^2 / \Omega_K (R_d)$ , where  $c_s$  is the sound velocity and  $\Omega_K$  is the Keplerian angular velocity, and we adopt  $\alpha = 0.01$ , as suggested by our SED modeling of CTTS disks (D'Alessio et al. 2001). Finally, the inclination-dependent flux of the rim is calculated as  $F_\lambda = I_\lambda A(i)$ , where the rim area  $A(i)$  has been derived from expressions in Appendix B in Dullemond et al. (2001). The specific intensity  $I_\lambda$  is calculated by integrating the temperature profile of the atmosphere (CMPD); in practice,  $I_\lambda$  differs from  $B_\lambda(T_{eff})$  by only a few percent. The location and height of the rim are highly dependent on the dust properties. To describe the dust opacity we take silicate abundances from Pollack et al. (1994), and a dust size distribution given by  $n(a) \propto a^{-3.5}$  between  $a_{min} = 0.005\mu\text{m}$  and a variable  $a_{max}$  (see D'Alessio et al. 2001 for details).

Given the stellar properties and  $L_{acc}$ , the emission from the rim depends on three parameters: the dust opacity, the dust destruction temperature, and the inclination. We have measured the *simultaneous*  $L_{acc}$  (i.e., derived from the same data as was the excess spectrum) for each object from the flux of the Br $\gamma$  line in each spectrum, employing the calibration of Muzerolle, Hartmann, & Calvet (1998). These values of  $L_{acc}$  are given in Table 1. The model parameters for  $R_d$ ,  $T_d$ ,  $a_{max}$ ,  $i$ , and  $q$  that provide the best fit to the dereddened

excesses are also given in Table 1; the emission from these models is shown in Figure 1. In general, the agreement between model and observation is excellent. The largest departure is observed at the longest wavelength for the object with one of the largest mass accretion rates in the sample (i.e. DR Tau). This is likely due to a contribution to the flux from the inner disk just outside the rim, which has not been included in our modeling. A few other objects show slightly larger fluxes than the models at long wavelengths, which in most cases is also likely due to emission from the disk just outside the rim. However, we note that the telluric absorption is especially strong in the  $M$  band, thus the flux discrepancies in some cases may also be due to uncertainties in the telluric cancellation.

The fits require small grains,  $\leq 1\mu\text{m}$ , in the atmosphere of the rim. This result is surprising in that much larger values of  $a_{max}$  are required to fit the median SED in Taurus (D’Alessio et al 2001), in agreement with flat slopes in the millimeter range. However, this may be an indication that dust settling has already taken place in the inner disk. Weidenschilling (1997) found that big grains settle to the disk midplane first, leaving behind a population of small grains.

The dust temperatures ( $T_d$ ) depend only on the shape of the excess spectra; most of the objects have  $T_d \sim 1400$  K. Sublimation temperatures of  $T_d \lesssim 1400$  K are expected given the central densities at the rim  $\lesssim 10^{-8}$  g cm $^{-3}$  (Pollack et al. 1994). We also find that  $T(2/3)$  is within  $\sim 100$  K from  $T_d$ , indicating that the rim atmosphere is nearly isothermal. Moreover, the rim heights are typically  $\sim 0.01 - 0.1$  AU and the ratio of the rim height to the scale height in all cases is  $\sim 4$ , in agreement with values for HAEBESs. (Dullemond et al. 2001). Note that our models are qualitatively similar to those of Natta et al. (2001) and Dullemond et al. (2001), but differ in several key respects. One, we include an atmosphere for the rim. Two, we take into account the wavelength dependence of the incident radiation field and the dust opacity (as in CMPD and Monnier & Millan-Gabet 2002). Three, and most importantly, we include  $L_{acc}$  as a heating source; inclusion of  $L_{acc}$  has important consequences for predicting the rim radius, as we discuss in the next section.

#### 4. Discussion

Our models of irradiated inner disk rims account for the large near-infrared excesses of CTTSs without requiring accretion rates that are too large. At the same time, the models explain the correlation between near-infrared excess and accretion rate found by MCH97, because the accretion shock radiation effectively increases the rim radiation.

Our models make several predictions that can be tested by further observations. One

of these is the inner radius of the dust disk; the best-fit values for each object are shown in Table 2. There is a two-fold increase of the rim radius (0.07 to 0.15 AU) for a factor of  $\sim 100$  increase in  $L_{acc}$ <sup>4</sup>. The two most luminous CTTSs in the sample, SU Aur and RY Tau, also have significantly larger rim radii (0.36 and 0.54 AU, respectively). In many cases the predicted inner rim radii produce near-infrared emission on spatial scales within reach of the capabilities of current interferometers. In fact, Akeson et al. (2002) estimated a size scale for the  $K$ -band emission from SU Aur of a few tenths of an AU, similar to our predicted value. Furthermore, just-published Keck interferometric observations of the CTTS DG Tau (Colavita et al. 2003) resolved the  $K$ -band emission and derived a radius of 0.12-0.24 AU. Using model parameters typical of the fits for our sample ( $q = 1$ ,  $\chi_d/\kappa_d = 2$ ,  $T_d = 1400$  K), and the known parameters of DG Tau ( $L_* = 1.07 L_\odot$ ,  $L_{acc} = 1.12 L_\odot$ ), we predict a rim radius of  $\sim 0.2$  AU, in excellent agreement with the Keck measurements. As we have already mentioned, models of dust sublimation have been used before in trying to explain interferometric observations of HAEBESs (Tuthill et al. 2001; Natta et al. 2001; Dullemond et al. 2001; Monnier & Millan-Gabet 2002). However, these models have not included the contribution from  $L_{acc}$ , and thus are likely to underestimate the emission sizes of most CTTSs. Future interferometric observations of CTTSs of a wide range of accretion and stellar luminosities should be able to confirm the relationships implied by our results.

Stars with the lowest  $L_{acc}$  have  $R_d$  close to or slightly larger than their corotation radii (see Table 1); however, as  $L_{acc}$  increases,  $R_d$  becomes much larger. Since all of these stars are accreting gas, and accretion can only occur if disk material extends all the way to or inside of the corotation radius, this then implies that stars with high  $L_{acc}$  have a dust-free pure gaseous innermost disk. Such a scenario is similar to our recent investigation of Herbig Ae stars (Muzerolle et al. 2003), where we combined a puffed inner dust rim with the D’Alessio et al. (1997) detailed accretion disk structure, using accretion rates estimated from UV fluxes or permitted line profile modeling. Because of the typically low values of the HAEBES mass accretion rates ( $\sim 10^{-8} M_\odot yr^{-1}$ ), the gas disk is either optically thin or else the height where the optical depth to the stellar radiation is unity is significantly reduced due to the lack of dust. This is also true for the CTTSs. Thus, the inner dust rim can still receive the direct stellar irradiation necessary to maintain its enhanced scale height. In the case of the hotter CTTSs presented here, the dependence of the inner dust rim radius on accretion is negligible since  $L_* > L_{acc}$ ; however, there must still be an inner gaseous disk to feed the accretion flows

---

<sup>4</sup>The dependence on accretion does not hold for DQ Tau, which has a much larger  $R_d$  than expected from its  $L_{acc}$ . This object is a spectroscopic binary with semi-major axis  $a \sim 0.067$  AU (Mathieu et al. 1997). If the circumbinary disk is truncated at  $\sim 2a$  (Artymowicz & Lubow 1994), then the truncation radius would be 0.13 AU, which is equal to our estimate for  $R_d$ . This suggests that the near infrared excess in DQ Tau corresponds to emission from the inner edge of the circumbinary disk.

onto these stars.

The inner dust rim model successfully accounts for all of the continuum excess veiling observed at  $K$  in CTTSs. This model may also explain the large near-infrared veiling observed in many protostars (Casali & Eiroa 1996; Greene & Lada 1996), as these objects probably have higher accretion rates (Muzerolle et al. 1998; Greene & Lada 2002).

Finally, the presence of a dust-free gas disk inside  $R_d$  in many CTTSs suggests that there may be difficulties for the X-wind model of chondrule formation (e.g., Shu et al. 2001), which invokes a wind arising from just outside the magnetosphere to lift solid particles out of the disk and carry them out to larger radii. If dust cannot exist in this region, which our results indicate is the case for the rapid accretion phases required by the X-wind model, then an alternative theory may be required to explain chondrule formation.

JM would like to thank John Rayner and Bobby Bus at IRTF for their able assistance with the SpeX observations and data reduction. This work was supported in part by NASA Origins of Solar Systems grant NAG5-9670.

## REFERENCES

- Akeson, R. L., Ciardi, D. R., van Belle, G. T., & Creech-Eakman, M. J. 2002, *ApJ*, 566, 1124
- Artymowicz, P. & Lubow, S. H. 1994, *ApJ*, 421, 651
- Bouvier, J., Cabrit, S., Fernández, M., Martín, E. L., & Matthews, J. M. 1993, *A&A*, 272, 176
- Calvet, N. & Gullbring, E. 1998, *ApJ*, 509, 802
- Calvet, N., Magris, G. C., Patino, A., & D’Alessio, P. 1992, *Rev. Mexicana Astron. Astrofis.*, 24, 27
- Calvet, N., Patino, A., Magris, G. C., & D’Alessio, P. 1991, *ApJ*, 380, 617
- Casali, M. M. & Eiroa, C. 1996, *A&A*, 306, 427
- Chiang, E. I. & Goldreich, P. 1997, *ApJ*, 490, 368
- Chiang, E. I. & Goldreich, P. 1999, *ApJ*, 519, 279
- Close, L. M., et al. 1998, *ApJ*, 499, 883
- Colavita, M., Akeson, R., Wizinowich, P. et al. 2003, *ApJ*, 592L, 83
- Cushing, M. C., Vacca, W. D., & Rayner, J. T. 2003, *PASP*, submitted

- D'Alessio, P., Calvet, N., & Hartmann, L. 2001, *ApJ*, 553, 321
- D'Alessio, P., Calvet, N., Hartmann, L., Muzerolle, J., & Sitko, M. 2003, in *Star Formation at High Angular Resolution*, ASP Conference Series, S-221, eds. M. G. Burton, R. Jayawardhana, & T. L. Bourke, in press
- D'Alessio, P., Cantó, J., Calvet, N., & Lizano, S. 1998, *ApJ*, 500, 411
- Dullemond, C. P., Dominik, C., & Natta, A. 2001, *ApJ*, 560, 957
- Eisner, J. A., Lane, B. F., Akeson, R. L., Hillenbrand, L. A., & Sargent, A. I. 2003, *ApJ*, 588, 360
- Folha, D. F. M. & Emerson, J. P. 1999, *A&A*, 268, 192
- Geene, T. P. & Lada, C. J. 2002, *AJ*, 124, 2185
- Gullbring, E., Hartmann, L., Briceño, C., & Calvet, N. 1998, *ApJ*, 492, 323
- Hartmann, L., Kenyon, S. J., & Calvet, N. 1993, *ApJ*, 407, 219
- Hartmann, L. & Stauffer, J. R. 1989, *AJ*, 97, 873
- Hillenbrand, L. A., Strom, S. E., Vrba, F. J., & Keene, J. 1992, *ApJ*, 397, 613
- Johns-Krull, C. M. & Gafford, A. D. 2002, *ApJ*, 573, 685
- Johns-Krull, C. M. & Valenti, J. A. 2001, *ApJ*, 561, 1060
- Mathieu, R. D., Stassun, K., Basri, G., Jensen, E. L. N., Johns-Krull, C. M., Valenti, J. A., & Hartmann, L. 1997, *AJ*, 113, 1841
- Meyer, M. R., Calvet, N., & Hillenbrand, L. A. 1997, *AJ*, 114, 288
- Millan-Gabet, R., Schloerb, F. P., & Traub, W. A. 2001, *ApJ*, 546, 358
- Monnier, J. R. & Millan-Gabet, R. 2002, *ApJ*, 579, 694
- Muzerolle, J., Calvet, N., & Hartmann, L. 2001, *ApJ*, 550, 944
- Muzerolle, J., D'Alessio, P., Calvet, N., & Hartmann, L. 2003, *ApJ*, submitted
- Muzerolle, J., Hartmann, L., & Calvet, N. 1998, *AJ*, 116, 2965
- Natta, A., Prusti, T., Neri, R., Wooden, D., Grinin, V. P., & Mannings, V. 2001, *A&A*, 371, 186
- Pollack, J. B., Hollenbach, D., Beckwith, S., Simonelli, D. P., Roush, T., & Fong, W. 1994, *ApJ*, 421, 615
- Rayner, J. T., Toomey, D. W., Onaka, P. M., Denault, A. J., Stahlberger, W. E., Watanabe, D. Y., & Wang, S.-I. 1998, *Proc. SPIE*, 3354, 468, *Infrared Astronomical Instrumentation*, ed. A. M. Fowler

Shu, F. H., Najita, J., Ostriker, E., Wilkin, F., Ruden, S., & Lizano, S. 1994, *ApJ*, 429, 781

Shu, F. H., Shang, H., Gounelle, M., Glassgold, A. E., & Lee, T. 2001, *ApJ*, 548, 1029

Weidenschilling, S. J. 1997, *Icarus*, 127, 290

Table 1. CTTS Sample & Model Parameters

Object	Sp. Type	$L_*$ ( $L_\odot$ )	$R_*$ ( $R_\odot$ )	$A_V$	$i_*$ ( $^\circ$ )	$R_{co}$ (AU)	$r_{2.2}$	$L_{acc}$ ( $L_\odot$ )	$R_d$ (AU)	$a_{max}$ ( $\mu\text{m}$ )	$T_d$ (K)	$i$ ( $^\circ$ )	$q$
DN Tau	M0	0.86	2.1	0.25	35	0.05	$0.2 \pm 0.2$	$<0.01$	0.07	0.1	1400	28	3.24
DQ Tau	M0	0.63	1.8	0.97	$23^a$	...	$0.3 \pm 0.2$	0.04	0.13	0.3	1000	17	1.39
BP Tau	K7	0.87	1.9	0.51	39	0.07	$0.6 \pm 0.2$	0.15	0.09	0.2	1400	26	1.65
DF Tau	M1	0.5	1.7	0.45	...	0.07	$0.8 \pm 0.3$	0.22	0.09	0.7	1300	61	0.98
UY Aur	K7	1.07	2.1	1.26	$42^b$	...	$1.5 \pm 0.5$	0.19	0.1	0.3	1400	67	1.31
DO Tau	M0	1.03	2.3	2.27	...	...	$2.0 \pm 0.5$	0.18	0.09	0.1	1400	63	2.55
DR Tau	K7:	0.87:	1.9:	1.6	69	0.08	$4.0 \pm 0.5$	1.01	0.15	0.5	1300	72	1.56
SU Aur	G2	12.9	3.5	0.9	72	...	$0.6 \pm 0.3$	1.47	0.36	0.2	1400	86	2.21
RY Tau	G5	12.8	3.6	1.8	...	...	$0.8 \pm 0.3$	4.04	0.54	0.3	1200	86	2.06

Note. — The stellar inclination angles,  $i_*$ , were estimated from  $v \sin i$  (Hartmann & Stauffer 1989),  $R_*$ , and the period (Johns-Krull & Gafford 2002, and references therein; Bouvier et al. 1993), except for: (a) taken from the Mathieu et al. (1997) estimate based on orbital components of the spectroscopic binary; (b) taken from the Close et al. (1998) estimate of the inclination of the circumbinary disk. Colons after the DR Tau stellar parameters indicate large uncertainty, due to the extremely strong optical veiling.  $R_{co}$  is the corotation radius, estimated from the stellar rotation rates. The rim model inclination angles,  $i$ , have uncertainties of  $\sim \pm 10^\circ$ .

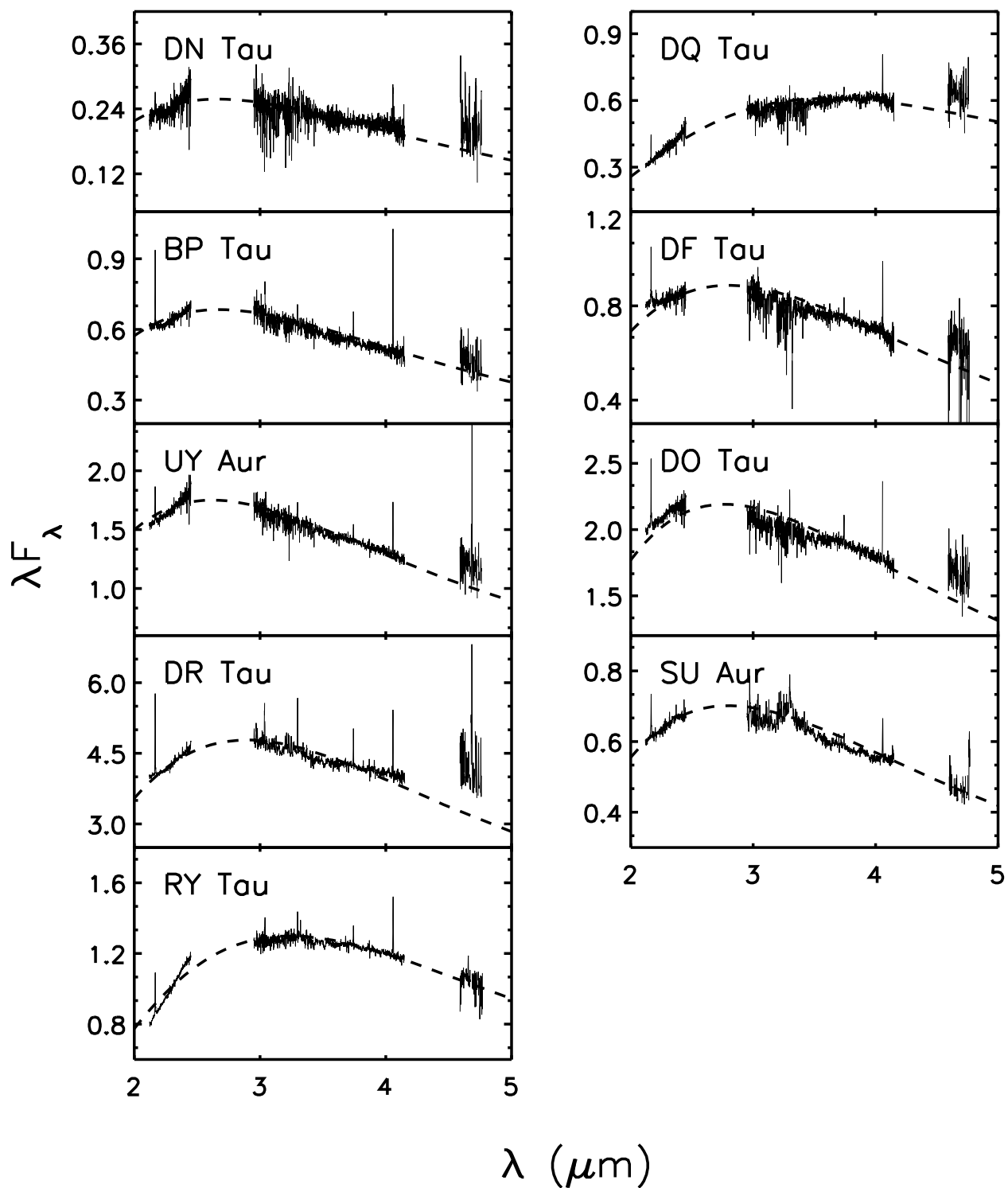


Fig. 1.— Near-infrared excess spectra of classical T Tauri stars. Each dereddened object spectrum has been subtracted by that of a dereddened weak T Tauri star of the same spectral type (with no excess). Apparent absorption features in the  $L$  and  $M$  bands are residuals from incomplete telluric cancellation. Prominent Brackett and Pfund emission lines, produced by accretion flows, can be seen in most of the spectra. The dashed lines show the emission from the best-fit inner dust rim models. Fluxes are in units of the photospheric flux at  $2.1 \mu\text{m}$ .